

Mobility Influences on the Capacity of Wireless Cellular Networks

Yide Zhang, Lemin Li, and Bo Li

ABSTRACT—Capacity has always been a major concern in wireless networks. This letter studies the impact of mobility on the overall system capacity in wireless cellular networks. In this letter, we present a simple system model which we developed to capture the inherent relationships among system capacity, new call blocking probability, handoff dropping probability, call terminating probability, and bandwidth utilization rate. We investigate the complex relationship between mobility and capacity-related parameters. Through simulation, we demonstrate that mobility has a significant impact on capacity and is reversely proportional to the bandwidth reserved for handoff traffic.

Keywords—Capacity, mobility, wireless cellular network.

I. Introduction

The capacity of a wireless cellular network is strongly related to the new call blocking probability (P_b) and handoff call dropping probability (P_d). Moreover, the call terminating probability (P_t) and system overall bandwidth utilization rate (BUR) are also of concern for carriers. We could express the capacity \mathcal{E} as

$$\mathcal{E}(P_b, P_d, P_t, R, \beta) = \frac{\lambda(P_b, P_d, P_t, R)}{\alpha \times R^2} \times \beta, \quad (1)$$

where β represents the BUR, $\lambda(P_b, P_d, P_t, R)$ is the traffic carried by a cell (in Erlang), R is the radius of the cell, and α is a normalized constant for the cluster size. The capacity can be expressed by $\lambda(P_b, P_d, P_t, R)$, in which the P_d specifies the QoS

guarantee, and P_b and R determine the overall system capacity. Existing research has shown that mobility affects these parameters [1]-[3]. T. Bonald and others [1] studied the mobility impact on flow level performance. C.T. Lea and others [2] illustrated that mobility and capacity can be viewed as equals using a simple example of a 4-cell system. In [3] and [4], the authors analyzed the impact of mobility on capacity in the context of wireless ad-hoc networks. To the best of our knowledge, there has been no conclusive study on mobility and capacity for wireless cellular networks. Due to its complex nature, there does not seem to be a simple linear relationship between mobility and capacity [5]. This letter aims to address this issue in a systematic way.

II. The System Model

In this study, we consider a wireless network with 49 homogeneous hexagonal cells with wrap-around. Guarded channel (GC) [5], [6] is employed. The system model includes a propagation model, a mobility model, a traffic model, handoff models, and other parameters. We focus on the mobility model and develop a simulation based on the parameters listed in Table 1.

Several parameters in the simulation follow standard propagation modeling. For instance, the distance-based propagation attenuation coefficient θ is used for modeling the distance-dependent fading, whereas standard deviation for shadow fading and shadow fading correlation are used to model the log-normal shadow fading.

Although mobility could be defined as the average number of handoffs during the lifetime of a call [2], we consider a more accurate mobility model in this letter. Following the layout of Fig. 1, we use a vector (X, Y) to represent the location of the user. We

Manuscript received June 06, 2006; revised Aug. 18, 2006.

Yide Zhang (phone: +86 28 83203008, email: computium@gmail.com) and Lemin Li (email: lml@uestc.edu.cn) are with the School of Communication and Information Engineering, the University of Electronic Science and Technology of China, Chengdu, China.

Bo Li (email: bli@cs.ust.hk) is with the Department of Computer Science, Hongkong University of Science and Technology, Hongkong, China.

Table 1. Parameters for simulation.

Number of clusters in the system (N)	7
Number of cells in each cluster (K)	7
Total cells	49
Number of channels in each cell (C)	variable
Guard channel threshold (C_G)	variable
Cell radius (R)	800 m
Number of sectors per cell	1 sector
Distance-based propagation attenuation coefficient (θ)	3.5
Thermal noise	-118 dBm
Standard deviation for shadow fading	6 dB
Shadow fading correlation	0.5
Sampling time interval	3 s
Average number of new call request to a cell (λ)	variable
Recorded average number of handoff call to a cell (γ)	variable
Mean holding time ($1/\mu$)	120 s
Mean speed	variable
Velocity correlation coefficient (ξ)	1
Handoff hysteresis (H)	3 dB
Call dropping SIR threshold	5 dB

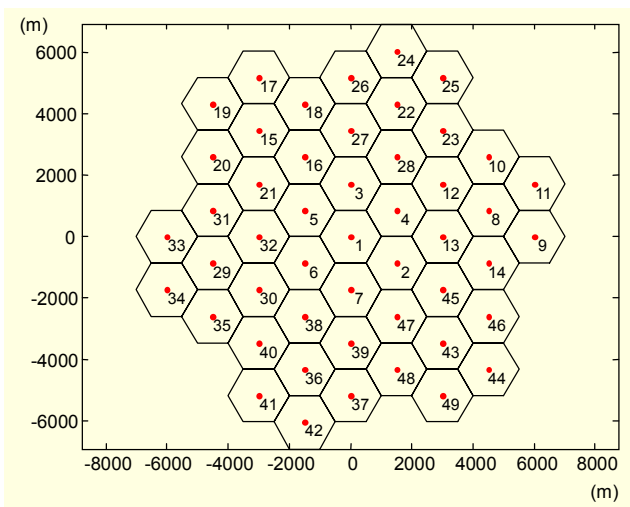


Fig. 1. System model.

decompose the user's mobility into V_x and V_y , which represent the velocity at the X - and Y -coordinates respectively, and V_x and V_y also jointly determine the trajectory direction of the user.

$$V_x(n) = V_x(n-1) \cdot \xi + \sqrt{1-\xi^2} \cdot V_{avg} \cdot \chi, \quad (2)$$

$$V_y(n) = V_y(n-1) \cdot \xi + \sqrt{1-\xi^2} \cdot V_{avg} \cdot \chi. \quad (3)$$

The current velocity of the user, both speed and direction, is defined as $V_x(n-1)$ and $V_y(n-1)$, whereas $V_x(n)$ and $V_y(n)$ are the next sample points. The predefined average velocity value is denoted by V_{avg} , while χ is an uncorrelated normal Gaussian variable with mean of 0 and deviation of 1, and ξ is the correlation coefficient of the velocity of a user between two successive sampling times.

III. Simulation Results and Discussion

The whole system model under consideration is plotted in Fig. 1. There is a total of 49 cells in the simulation. Wrap-around is applied, rendering the out-going calls returning from the other side of the network. The simulations are based on Matlab, and a few functions are revised from the simulation software in [7].

The overall system capacities are significantly related to P_b , P_d , P_s and BUR. We use the binomial distribution to approximate the arrival of the new calls. The recorded average value of λ is 1.6 calls per cell per sample (3 s). The service rate is exponentially distributed with a mean holding time $1/\mu$ of about 120 s [5]. We assume that C_G is in a range between 0 and 6 and we limit P_t to a range between 0.2% and 0.4%. Furthermore, the mobility varies. The average velocity V_{avg} spans from 0.1 mps (meters per second) to 50 mps, with fixed steps of 1 mps (Table 2). User trajectory can be calculated by (2) and (3).

Figures 2, 3, and 7 depict the system performance measurement parameters (BUR, P_b , and P_d) against mobility variation when there is no GC; whereas, Figs. 4 through 6 present the situations with GC. The mobility cases selected from Table 2 for GC situations start with mobility case 1, and then span from 10 to 50 mps, with fixed steps of 10 mps. We ran the simulation multiple times for a sufficient duration until the system reached a steady state. In the figures, each plotted point represents the average of the recorded data.

In order to obtain reasonable values of blocking and dropping probabilities, we kept the BUR within a range from 88% to 92% (Fig. 3) when there was no GC and within a range from 82% to 90% (Fig. 5) in cases with GC. Apparently, In order to obtain reasonable values of blocking and dropping probabilities, we kept the BUR within a range from reserving more channels for handoff calls decreases the BUR.

Table 2. Adopted mobility values.

Mobility cases	1	2	3	4	5	...	50	51
Velocity-mps	0.1	1	2	3	4	...	49	50
Velocity-kph	0.36	3.6	7.2	10.8	14.4	...	176.4	180

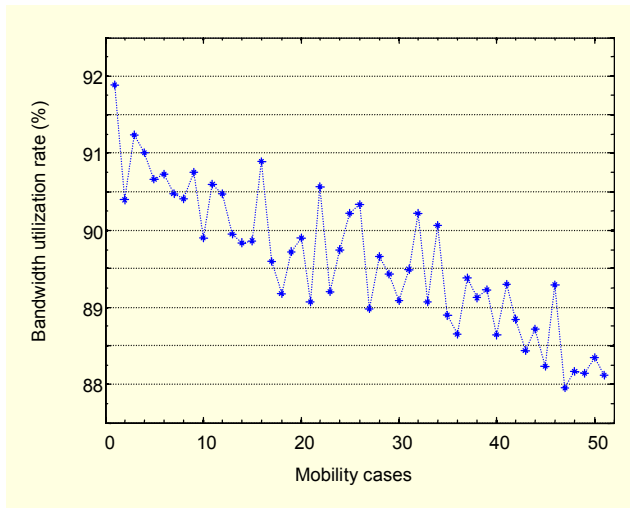


Fig. 2. Mobility vs. whole system BUR.

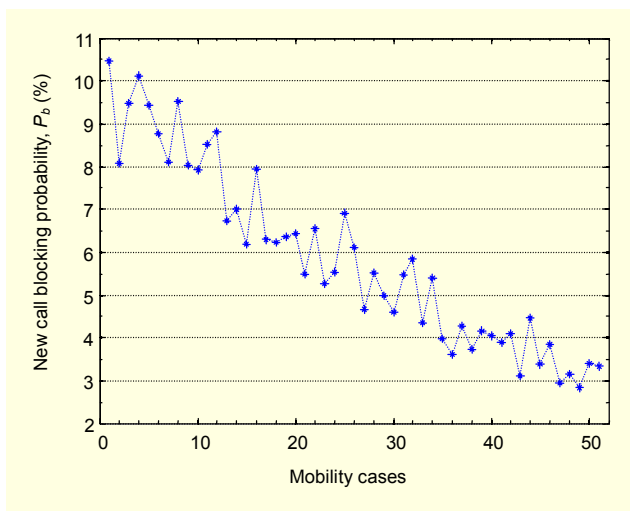


Fig. 3. Mobility vs. new call dropping probability.

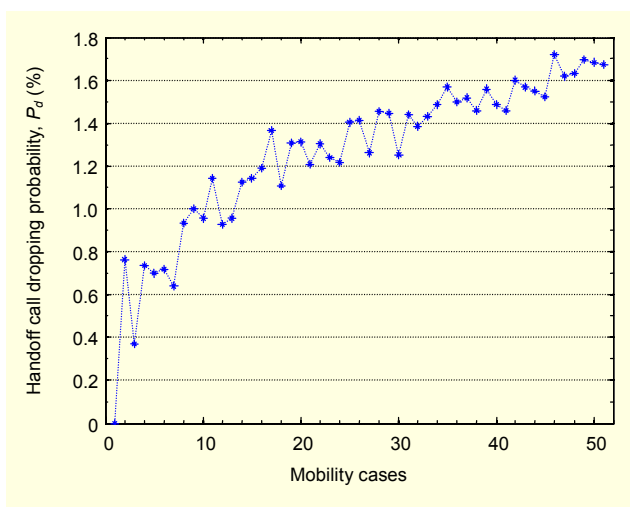


Fig. 4. Mobility vs. handoff call dropping probability.

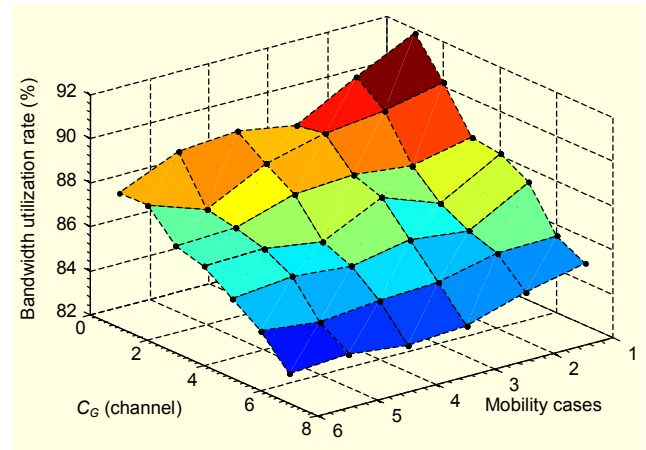


Fig. 5. Whole system BUR for varying C_G .

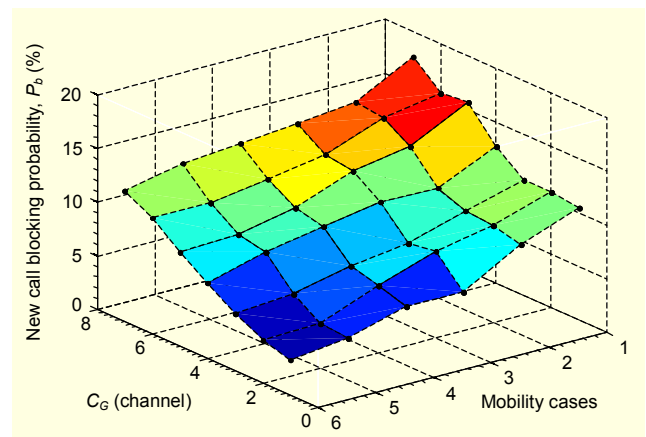


Fig. 6. New call blocking probability for varying C_G .

The mobility increase demonstrates great impact on the BUR, P_b , and P_d . Higher mobility implies a lower BUR and P_b , and a higher P_d . When the BUR and P_b decrease with the increment of mobility with large granularity, the values of the BUR and P_b oscillate with small granularity, implying a large variation of Rayleigh fading. Noticing that P_d has the opposite trend of BUR and P_b when mobility increases; in high mobility cases, the change of P_d is more stable than that in low mobility cases.

Under the conditions of high mobility, that is, in the mobility cases above case 30 in Table 2, the P_d rises from about 1.4% to 1.7% with a performance loss of 17.6% (Fig. 4), whereas the P_b falls from 5.5% to 3% with a performance improvement of 83.3% (Fig. 3), and the BUR only loses 1.7% on average (from 89.5% to 88% as shown in Fig. 2). If the P_b receives the same weight as the P_d , we observe a significant increase of the overall system capacity ε in (1) under the conditions of high mobility.

On the other hand, for low mobility cases below case 10 in Table 2 when the P_d is low enough, the BUR falls from about 92% to 90.5% with a performance loss of 1.6%, but a

performance gain in the P_b is notable, with a performance improvement of more than 31%. Even for a system with greater P_d concerns, the overall system capacity ε will benefit from mobility increase when user movement patterns change from pedestrian to low velocity vehicles.

The same effects can also be observed when there is GC. The increase in mobility slightly reduces the BUR, but significantly reduces the P_b , at the expense of an acceptable increase in P_d . However, when the P_d is finely controlled below 2% (Fig. 7), the increase in mobility is reflected by a notable decrease in P_b , from more than 15% to 4% (Fig. 6). While the slight increase in P_d reduces the traffic carried λ by a cell as in (1), the notable decrease in P_b increases the traffic carried λ significantly as the system capacity ε in (1) ultimately allows the system to accommodate more new users.

We observe that the increase in mobility and the decrease in P_b provide an opportunity to allocate the released channels from out-going handoff calls to new calls. There is also a chance that some of the calls could finish within the given period of time and release the occupied channels for other new calls or handoff call requests from neighboring cells. The low mobility scenario does not seem to be able to combat the harmful “hot-spot” situation effectively, in which any uneven load distribution can quickly lead to performance degradation. This even can occur in a single cell, which can potentially decrease system capacity significantly. On the other hand, higher mobility can introduce more handoffs, while it also provides opportunities to more evenly distribute the traffic among all cells. Generally speaking, mobility increases the overall system capacity of the wireless cellular network.

Another conclusion which can be drawn for the GC scheme (Figs. 5-7) is that mobility is reversely proportional to the bandwidth reserved for handoff traffic. When the BUR and P_b decrease with the increase in mobility, the change of c has a

negative impact on the BUR and P_b , reducing the BUR and increasing the P_b significantly. On the other hand, while the P_d oscillates with the increase in mobility, the increase in C_G reduces the P_d . Hence the impact of mobility on the BUR resembles that of C_G , whereas increasing mobility neutralizes the influences on the P_b and P_d caused by the increment of C_G . High mobility reduces the advantage gained from adding more C_G .

Therefore, we could conclude that mobility in general can increase the overall system capacity of wireless cellular networks. The significance of such change is determined by the degree of mobility, and by the channel reservation under the GC scheme.

IV. Conclusion

In this letter, we demonstrated that mobility has a great influence on the capacity of wireless cellular networks. We showed that the parameters P_b , P_d , P_b , and BUR vary when mobility changes, but the degrees of variation are correlated and differ under the varying conditions of high and low mobility. Generally speaking, from simulation and mathematical derivation, we conclude that mobility increases the system capacity of wireless cellular networks. Under the GC mechanism, we show that the channel reservation should be dynamically adjusted by incorporating the mobility parameter.

References

- [1] T. Bonald, S.C. Borst, and A. Proutiere, “How Mobility Impacts the Flow-Level Performance,” *Proc. IEEE INFOCOM 2004*, Hongkong, China, 2004, pp. 1872-1881.
- [2] C.T. Lea and M Zhang, “On the Mobility/Capacity Conversion in Wireless Networks,” *WCNC’03*, vol. 3, 2003, pp.1433-1438.
- [3] M. Grossglauser and D. Tse, “Mobility Increases the Capacity of Ad_hoc Wireless Networks,” *IEEE/ACM Trans. Networking*, vol. 10, no. 4, Aug 2002, pp. 477- 486.
- [4] S.A. Jafar, “Too Much Mobility Limits the Capacity of Wireless Ad Hoc Networks,” *IEEE Transactions on Information Theory*, vol. 51, Nov. 2005, pp. 3954-3965.
- [5] B. Li, L.-Z. Li, B. Li, K. Sivalingam, and X.-R. Cao, “Call Admission Control for Voice/Data Integrated Cellular Networks: Performance Analysis and Comparative Study,” *IEEE J. Selected Areas in Communications, Special Issue on: All-IP Wireless Networks*, vol. 22, no. 4, May 2004, pp. 706-718.
- [6] C.T. Chou and K.G. Shin, “Analysis of Adaptive Bandwidth Allocation in Wireless Networks with Multilevel Degradable Quality of Service,” *IEEE Trans. Mobile Computing*, vol. 3, no. 1, Jan.-Mar. 2004, pp. 5-17.
- [7] J. Zander and S.L. Kim, *Radio Resource Management for Wireless Networks*, Artech House, Norwood, USA, 2001.

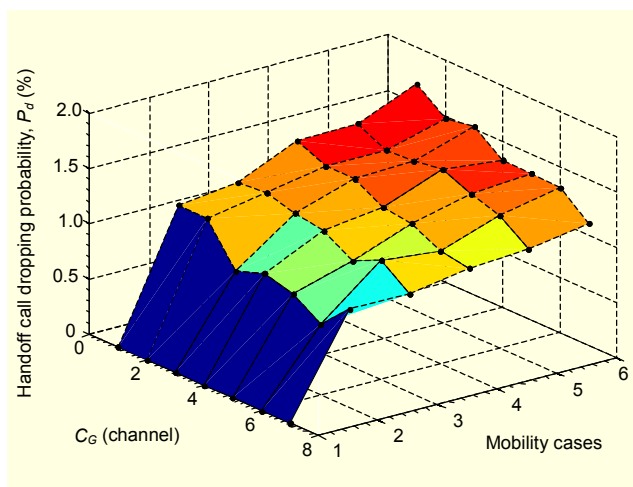


Fig. 7. Handoff call dropping probability for varying C_G .